

Variations in Balmer-line Stark profiles with atom-ion reduced mass

W. L. Wiese, D. E. Kelleher, and V. Helbig*

Institute for Basic Standards, National Bureau of Standards, Washington, D.C. 20234

(Received 13 February 1975)

Calculations of the Stark broadening of hydrogen lines treat the radiating atoms and the perturbing ions as quasistatic. The present experiment represents an attempt to determine whether the possible breakdown of this approximation near the center of the line can account, at least partially, for the existing discrepancies between theoretical and experimental profiles in the core of the Balmer lines. The central regions of H_α , H_β , H_γ , and H_δ profiles have been measured in a wall-stabilized arc over a range of atom-ion relative velocities by varying the atom-ion reduced mass. The cores of all four lines exhibit a significant dependence on the reduced mass. With increasing reduced mass, the experimental profiles gradually show more structure, but still less than the theories predict. Extrapolation of the results for H_α and H_β to infinite reduced mass, i.e., to the static case, gives results that agree quite well with recent calculations.

I. INTRODUCTION

Two recent experimental investigations on the broadening of hydrogen Balmer lines by plasmas have yielded as one of their principal results an appreciable disagreement with the theory for the regions near the line centers. The theoretically predicted profiles¹⁻³ exhibit significantly more structure than is experimentally observed.^{4,5} One of several reasons proposed for this discrepancy⁶ is the possible breakdown near the line center of the approximation of static ions (the quasistatic approximation) made by present theories. Effects of ion motion may be tested experimentally by employing atomic radiator-perturber combinations of different reduced masses at approximately constant plasma conditions or by variation of the plasma temperature for constant reduced mass and electron density.

In an earlier experiment,⁷ it was observed by two of us that the central minimum of H_β deepened toward the theoretical value as the reduced mass μ of the radiating-atom-perturbing-ion system was increased. The relative minimum (with respect to the peak) was observed to scale approximately as $1/\sqrt{\mu}$ for a fixed electron density. Values of the relative minimum extrapolated to the static case ($\mu = \infty$) yielded values only slightly smaller than theoretically predicted.

In this paper we report results for three other Balmer lines: H_α , H_γ , and H_δ . For the sake of completeness, we have also included a brief review of our earlier results for H_β and detailed comparisons with all other experiments.

II. EXPERIMENTAL DETAILS

A steady-state axially symmetric plasma is generated by a wall-stabilized arc. A current-regu-

lated 150-kW dc power supply is used to drive the arc in the current range from 20 to 100 A within a tolerance of about 0.3%. A schematic diagram of the arc is given in Fig. 1. Stacks of insulated water-cooled copper disks are used to form a central channel about 10 cm long and from 2 to 5 mm in diameter, depending on the plasma (a narrow channel is particularly required for wall stabilization of pure hydrogen).

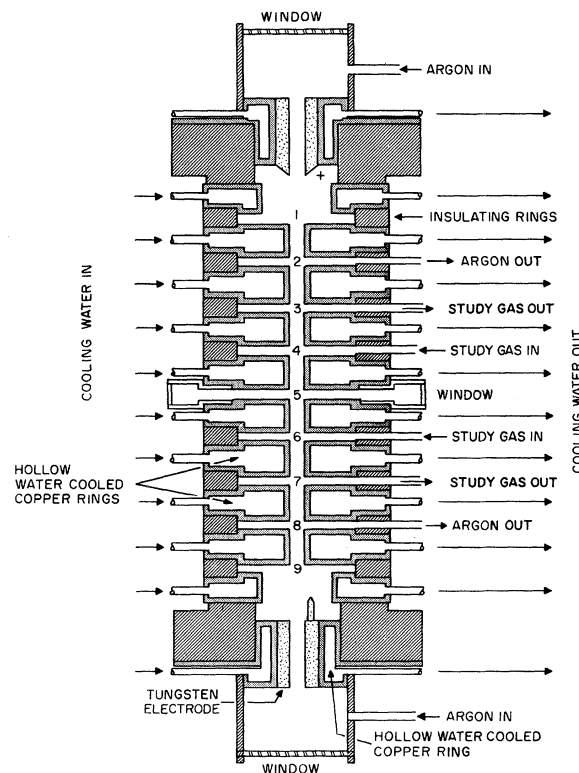


FIG. 1. Schematic diagram of the wall-stabilized arc.

To avoid self-absorption, measurements of pure hydrogen and deuterium were made side-on through the window at the center of the arc. At each wavelength a continuous scan is made across the arc which is mounted and translated on a lathe. The signal from the photomultiplier tube is amplified and integrated continuously over 50 1-sec intervals. The data is stored on tape and subsequently Abel-inverted⁴ to yield relative intensities at discrete radial positions. A computer code corrects the raw data for finite integration time and fits them to a 12-term Legendre polynomial with odd terms included. The inversion is then performed analytically about the center of the fitted curve.

End-on observations down the central axis of the arc were performed with a small amount of hydrogen or deuterium in a carrier gas. As indicated in Fig. 1, a blanket of the pure carrier gas, most frequently argon, was maintained in the regions of the electrodes (Secs. 1 and 2, and 8 and 9 in Fig. 1). This assured that the hydrogen lines were emitted only from the homogeneous central region (Secs. 3-7) of the arc. The end-on data for H_α were integrated for 0.5-sec intervals, with about 250 points taken over the profile and stored on tape. Self-absorption measurements were made end-on by collecting the light passing through the back end of the arc with a spherical mirror and refocusing it back onto the arc axis. The optical depth τ is equal to $\ln[(A-1)/(B-1)]$, where A is the ratio of the signals with and without the reflected light included, measured at an optically thin region of the spectrum, and B the ratio at the wavelength where τ is desired to be measured. This expression is exact for the case in which, along the line of sight, the temperature is uniform, even if the absorption coefficient varies due to concentration changes.

A 2.25-m Ebert monochromator with a 1800-line/mm grating was used for these measurements. Its apparatus profile was determined with a mercury low-pressure discharge lamp, and the half-width measured to be 0.1 Å in first order with optimal slit settings.

No absolute intensity measurements were made. The electron density has been determined from the Stark half-width of the Balmer line under study, utilizing previously measured⁴ relationships between electron density and half-width. A precise value of the temperature is not required for this study. In general, the temperature has been determined from the plasma equilibrium relations by assuming local thermodynamic equilibrium. A more extensive discussion of the temperature and density determination, as well as of the arc and data collection system, is given in Ref. 4.

III. H_α

A. General remarks

The "unified" theory of Vidal, Cooper, and Smith¹ (VCS) yields a much more pronounced peak than is observed experimentally.^{7,8} Calculations based on a generalized impact approximation by Kepple and Griem² (KG), on the other hand, predict much less structure than is observed. The large difference between these two theories at the peak of H_α is due mainly to the fact that the unified theory retains the upper-lower state interference term, while the Kepple-Griem theory does not. There is still disagreement^{1,2,9} as to whether or not this term should be retained. A recent refinement of the unified theory by Roszman¹⁰ indicates that the inclusion of time ordering (to all orders) substantially reduces the discrepancy. An overview of the present situation is seen in Fig. 2, where the theories are compared with our measurements. Roszman's calculated peak is still on the order of 20% higher for hydrogen than the measured one, while the remainder of the profile is in excellent agreement with the experiment. All profiles in Fig. 2 have been normalized to unit area and correspond to an electron density of about $6.4 \times 10^{16} \text{ cm}^{-3}$.

The two experimental profiles in Fig. 2 were measured end-on in a 3-mm-diameter wall-stabilized arc operated in argon with approximately 0.3% admixtures of hydrogen and deuterium, respectively. It is seen that as the radiator-perturber reduced mass [$\mu = m_r m_p / (m_r + m_p)$] is increased from $\mu \approx 1$ to $\mu \approx 2$, agreement with the most recent theoretical profile by Roszman¹⁰ improves. A more quantitative presentation of these results will be given after the following discussion of experimental points critical to their measurement.

B. Critical experimental factors

1. Matching electron densities for H_α and D_α

The electron density N_e was determined from the Stark half-width of H_α , using an experimentally determined relation between width and density.⁴ Precise (i.e., better than 10%) values of N_e were not required for this study. However, it was critically important that N_e be the same for the measurement of both the hydrogen H_α and deuterium D_α profiles. To this end, the argon continuum level at 5320 Å was made equal for both the small hydrogen and deuterium admixtures. This was done by fine adjusting the current of the "deuterium" arc until its continuum matched that of the hydrogen case. The continuum intensity has been chosen since it depends on the square of N_e . The selected wavelength is in a convenient spectral range, free of spectral lines. The electron density was observed to re-

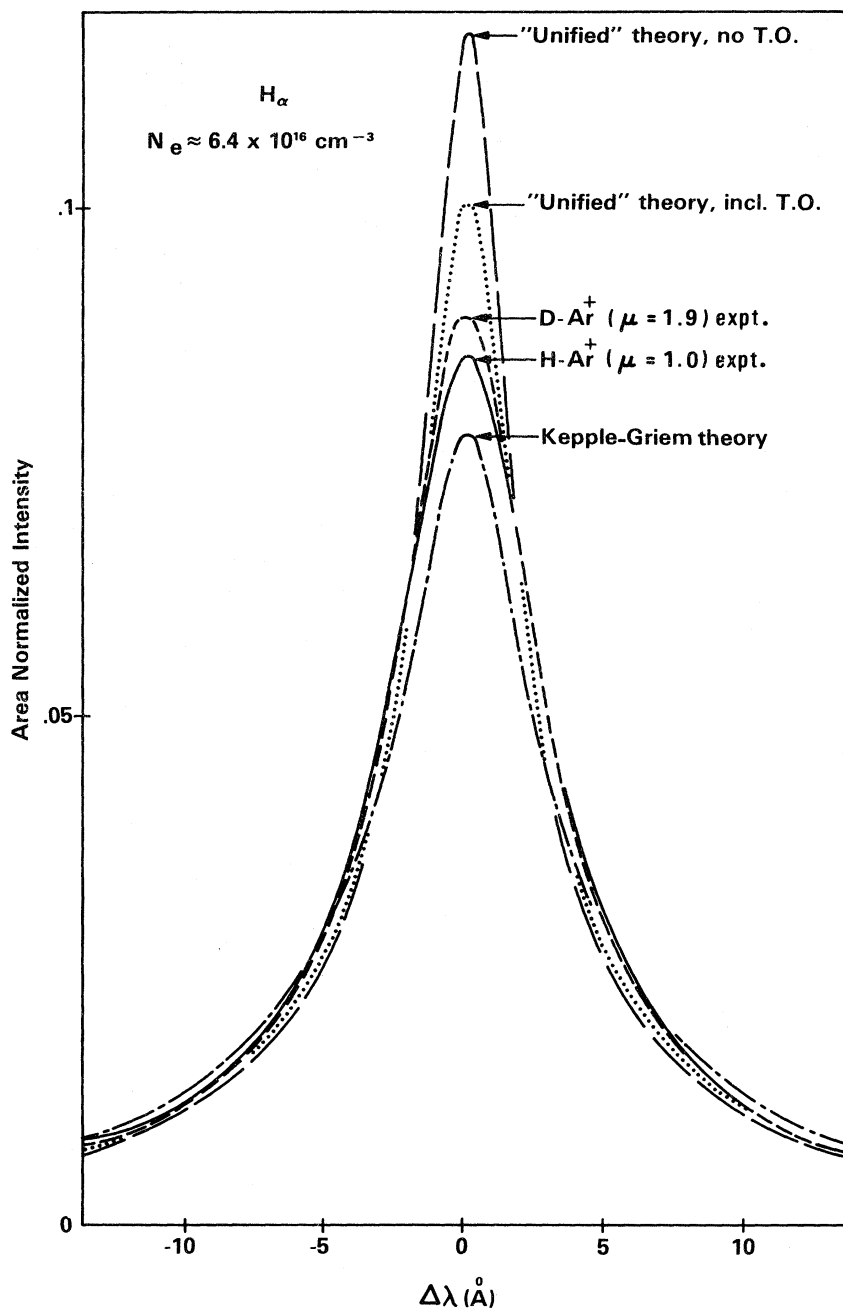


FIG. 2. Theoretical and experimental H_{α} profiles for $N_e = 6.4 \times 10^{16} \text{ cm}^{-3}$, $T = 12000 \text{ K}$. All profiles are area normalized. The large difference at the peak between the "unified" theory (Ref. 1) [time ordering (T.O.) not included] and the Kepple-Griem theory (Ref. 2) is mainly due to the fact that the unified theory retains the upper-lower state interference term, while the latter does not. The profile of Roszman (Ref. 10) takes time ordering into account for the unified theory. Each experimental profile represents an average of three scans, each scan having approximately 250 points over the profile.

spond quite sensitively to variations in the small admixtures, especially for $N_e < 6 \times 10^{16}$. The photomultiplier was left under voltage for several days to assure constant sensitivity; this was directly checked by making periodic remeasurements, during a run, of the pure-argon continuum level at a fixed current. While the absolute value for N_e is estimated to be uncertain to about 10%, we were able to assure that N_e was the same for both the hydrogen and deuterium measurements to within better than 1%.

2. *Requirement of small optical depth.* The optical depth of the H_{α} (D_{α}) peak was measured to be 0.1 or less, depending primarily on the H (D) concentration. The measurement was done with the previously discussed optical arrangement, in which a concave mirror in the extension of the optical axis focuses the light back into the plasma. The small first-order correction which was made for optical depth may be expressed as $I'(\lambda) = I(\lambda)/[1 - \tau(\lambda)/2]$, where $I(\lambda)$ is the total measured intensity (including continuum) at wavelength λ

and $\tau(\lambda) = \tau(\text{peak})I(\lambda)/I(\text{peak})$. $\tau(\text{peak})$ is the optical depth measured at the peak of the line, and $I'(\lambda)$ is the corrected intensity. As a further precaution, the concentration of deuterium in argon was adjusted until the D_α peak matched that of the previously measured H_α peak. In this way, any error in the measurement of the optical depth would effectively cancel in the comparison of the hydrogen and deuterium profiles.

3. *Stark-profile purity.* For the chosen experimental conditions, Stark broadening dominates. While the observed line profiles could also be influenced by other broadening mechanisms as well as instrumental broadening, numerical estimates show that the profiles are virtually pure Stark profiles for all but the lowest electron density. In this case a 1% correction in the relative width and peak difference was required due to the Doppler width, which was 0.5 \AA for hydrogen and 0.35 \AA for deuterium. The apparatus width, which was set to 0.2 \AA for H_α , as well as van der Waals and resonance broadening,¹¹ were always negligible. For the other Balmer lines, the Stark profiles are much broader, so that other broadening mechanisms could be neglected entirely.

4. *Spatial resolution and homogeneity of plasma.* Sufficient spatial resolution and plasma homogeneity was achieved in the end-on observations by using an $f/140$ optical system with a hydrogen- (or deuterium-) argon plasma of 40-mm length. In this arrangement, with $100 \mu\text{m}$ slits and a 2:1 image-to-object ratio, a nearly uniform plasma column of about 0.15-mm radius along the center arc axis is observed. Pure carrier gas, i.e., pure argon, is used near the electrode regions, so that hydrogen (or deuterium) is confined to the homogeneous central part of the arc column (Secs. 3–7 of Fig. 1). Of course, there remains a gradient of T and N_e in the transition layer between the pure carrier gas and the mixture. In our case, however, such gradients were very small since, e.g., the transition is from a region with about 99.7% argon to one with 100% argon, with all other factors kept constant.

5. *Continuous background under the line.* The continuum under H_α and D_α was determined in a pure-argon arc. As with deuterium, the current was adjusted until the argon continuum at 5320 \AA matched that measured with the small hydrogen admixture. The pure-argon-continuum measurement was made in between the hydrogen and deuterium measurements.

6. *H_α and D_α line wings.* The intensity distributions in the far wings, required for area normalization, were estimated by extrapolating our outermost points using an asymptotic Holtsmark wavelength dependence^{1,2} ($C\Delta\lambda^{-5/2}$, where C was chosen

to match the outermost data points). For both hydrogen and deuterium, the wings contributed about 10% to the area.

7. *Effects of isotopic impurity.* The elimination of isotopic impurities, i.e., a deuterium admixture free of any hydrogen impurity and vice versa, is very important since the centers of H_α and D_α differ in wavelength by 1.8 \AA . The impurity was estimated from the peak of the residual line not to exceed 5% of the 0.3% admixture. This contribution was subtracted out as part of the continuum.

C. Results

In Fig. 3 are plotted the (full) half-width and inverse of the peak height (arbitrary scale) of the area-normalized profiles versus N_e on a log-log scale. The straight lines represent a least-squares fit through the data. All the points for the H_α widths fall exactly on a line by construction, since a straight-line relationship was used to derive N_e from the H_α widths. The average deviations of the data points from the fitted curves are 0.3% for the inverse peak of H_α , 0.7% for the half-width of D_α , and 1.6% for the peak of D_α . The standard errors of the slopes of the fitted curves turned out to be essentially the same as the above figures. The larger uncertainties for the D_α points are probably due largely to the random error in setting the electron density of the deuterium measurement equal to that of hydrogen. The peak values are understandably less precise than those for the widths, since they reflect uncertainties in the area normalization, which do not affect the widths.

In Fig. 4 the relative differences between the

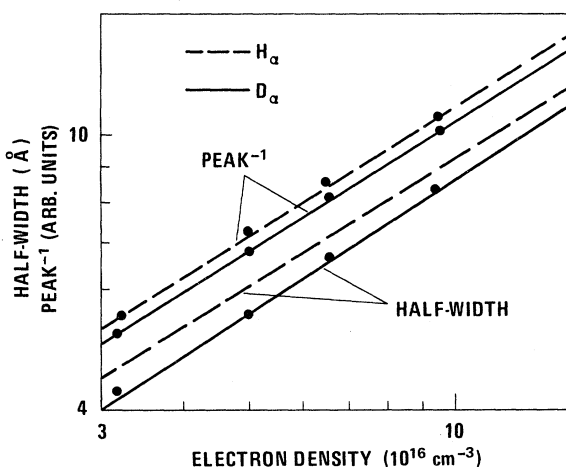


FIG. 3. Half-width and inverse peak versus electron density for H_α and D_α . The half-width data for hydrogen fall identically on the dashed line by construction, since the electron density was determined from the measured half-width of H_α . The best-fit curves in this figure were used to generate the curves in Fig. 4.

half-widths of hydrogen and deuterium have been plotted versus N_e . The relative differences in the peaks are also presented. The curves were generated using the best-fit curves of Fig. 2. The electron-density dependence of the differences in half-width appears fairly well determined, while for the peak differences one may only state qualitatively that they are distinctly smaller than those for the half-widths. This suggests that the H_α and D_α profiles differ in character; if, for example, both profiles were of the dispersion type with the same area, then the relative difference in peak heights would be equal (and opposite) to that for the half-widths.

An extrapolation of the experimental H_α results to $\mu = \infty$ is of considerable interest since this is the case for which the theoretical calculations have been made; i.e., the perturbing ion is treated as stationary with respect to the atom. In a previous experiment,⁷ the "dip" of H_β measured at $\mu \approx \frac{1}{2}$, 1, and 2 was observed to scale linearly as $1/\sqrt{\mu}$. For H_α , the $\mu = \frac{1}{2}$ (pure hydrogen) case could not be measured because of the self-absorption problem. Since effectively only two data points ($\mu \approx 1$ and 2) are available, it has not been possible to determine the μ dependence of the H_α data. We have therefore simply assumed the same $1/\sqrt{\mu}$ dependence in extrapolating the H_α half-width data to

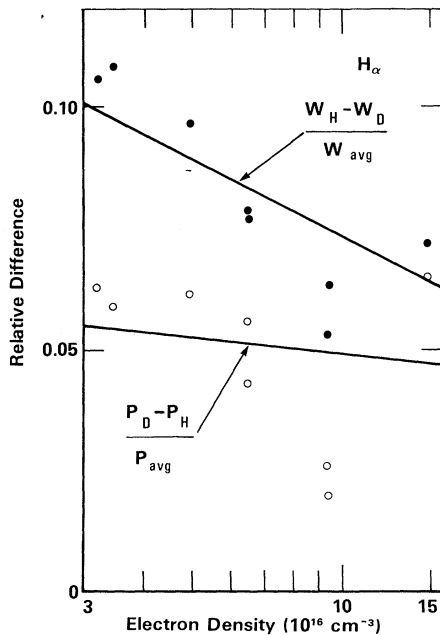


FIG. 4. Relative differences in the half-widths and peaks of H_α and D_α versus electron density. The data are taken from two independent runs. The straight lines through the data were generated from the curves in Fig. 3.

$\mu = \infty$. The results of this extrapolation at several different electron densities are included in Fig. 5, where the electron density is plotted versus half-width on a log-log scale. Also presented in this figure are the experimental data for $\mu \approx 1$ ($H\text{-Ar}^+$) and $\mu \approx 1.9$ ($D\text{-Ar}^+$), as well as the theoretical data of Kepple and Griem,² the unified theory without time ordering,¹ and the unified theory with time ordering included.¹⁰ The electron-density dependence of the measured half-widths is seen to change slightly with reduced mass, and the slope of the extrapolated data approaches the slopes of all three theoretical curves, which are quite similar to one another.

The four extrapolated data points ($\mu = \infty$) scatter about the theoretical curve of Roszman, i.e., the unified theory including time ordering. This agreement over the whole measured range of electron density is indeed remarkable, though the fact that the agreement is as good as it is may be fortuitous. While the extrapolated experimental results should be treated with caution, it seems nevertheless reasonable to conclude from the results in Fig. 5 that ion dynamic or "reduced-mass" effects play a significant role in the core of H_α .

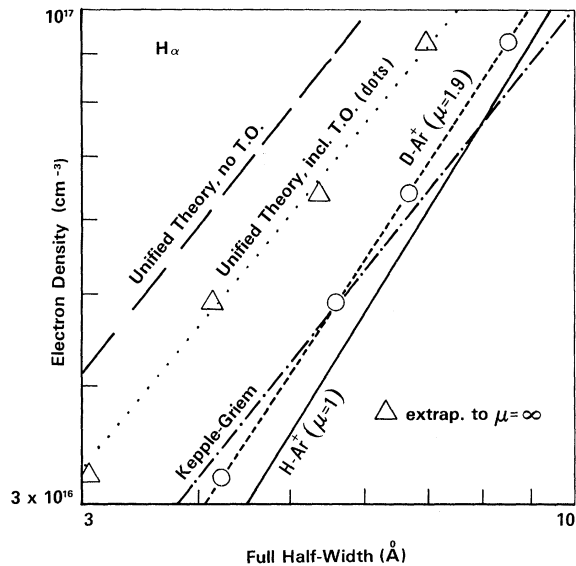


FIG. 5. Electron density versus half-width of H_α . The solid line, $H\text{-Ar}^+$, is taken from previously measured data (Ref. 4). The H_α half-widths measured in the present experiment were used to determine the electron density according to these results. The half-widths of D_α in argon ($\mu \approx 1.9$) were measured at these same electron densities (see text). The triangles represent an extrapolation of the experimental data to $\mu = \infty$, assuming a $1/\sqrt{\mu}$ dependence. The temperatures for both the theoretical and experimental curves range from 10 800 K at $N_e = 3 \times 10^{16}$ to 12 500 K at $N_e = 1 \times 10^{17}$.

IV. H_β

A. General remarks

Unlike H_α (and H_γ), H_β has no central unshifted Stark component, and therefore exhibits a dip or minimum in the center. Many experimental studies and applications of the H_β profile have been made, and in general, good agreement with calculated profiles has been found, but again with the marked exception of the region at and near the central minimum. The dips in high-density hydrogen plasmas have been measured to be about 15%, while the calculated ones are about 40% (for the Roszman, as well as VCS and KG calculations). [The dip is here defined to be the quantity (peak - minimum)/peak, where the peak is the average of the two maxima.] To test for ion dynamic effects in the H_β line center, we carried out a series of measurements of the dependence of the central minimum on the radiator-perturber reduced mass, which we reported earlier in a letter.⁷ The results of these measurements are summarized below and are now also compared with data obtained recently by other authors.^{5,12-17} (Since we discussed the critical experimental factors in the earlier paper, we shall not repeat this discussion here, but want to point out that in the H_β measurements the critical factors are much less sensitive than for H_α since no area normalization is involved and the H_β dip is only weakly dependent on electron density.)

B. Correlation of central minimum with reduced mass

The H_β central minimum was found to be correlated to the radiator-perturber reduced mass rather than, for example, the mass of the perturber alone. Seven different radiator-perturber combinations having essentially the same reduced mass ($\mu \approx 1$) were measured to have the same dip, within the experimental uncertainty. These included a pure-deuterium plasma as well as 4% (atomic) admixtures of hydrogen to Ne, Ar, Kr, Xe, N, and O plasmas. Radiator-perturber combinations corresponding to two different reduced masses resulted in H_β dips that were distinctly different, one larger—one smaller. These were pure hydrogen ($\mu = 0.5$) and an admixture of deuterium to argon ($\mu \approx 2$).

Figure 6 contains the central portion of three H_β profiles corresponding to different values of μ . All profiles were measured at approximately the same electron density, $N_e \approx 8 \times 10^6 \text{ cm}^{-3}$, and have been normalized to agree at the half-width and average peak of the line. As the reduced mass increases, the dip becomes more pronounced and approaches that of the theory.

The relative minimum of H_β was found to scale linearly as $1/\sqrt{\mu}$ at fixed electron density over the measured range of $\mu = 0.5$ to $\mu = 2$. In Fig. 7 the dip is plotted versus $1/\sqrt{\mu}$ at three different electron densities. The dashed lines indicate an extrapolation to the static-particle case ($\mu = \infty$). While the validity of this rather extended extrapolation is, of course, somewhat questionable, it is nevertheless of interest to compare the extrapolated values to the theoretical ones, which are calculated treating the radiating atoms and perturbing ions as static. This comparison can be seen in Fig. 8, which is updated and extended from our previous paper.⁷

C. Electron-density dependence

The electron-density dependence of the relative minimum was observed to change appreciably for different fixed μ . As can be seen in Fig. 8, the slope of the dip versus N_e even changes sign between the $\mu = 0.5$ and the $\mu = 2$ case. As μ increases

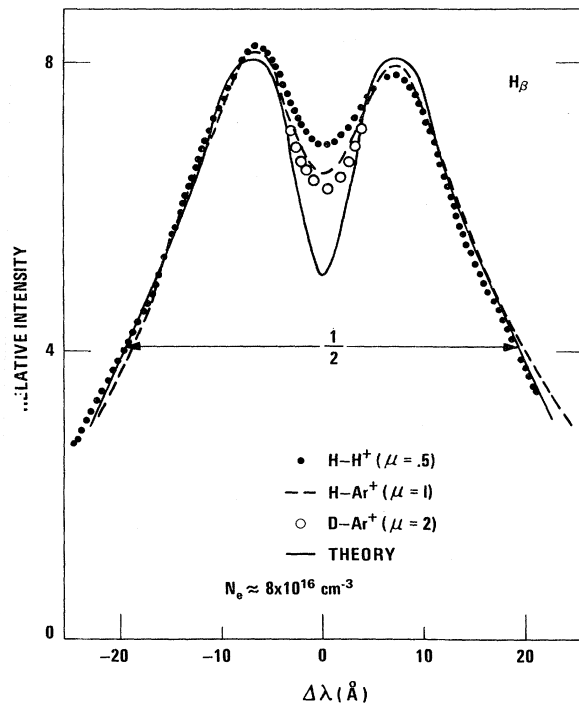


FIG. 6. Central part of the H_β profile at three different values of the reduced mass for $N_e \approx 8 \times 10^6 \text{ cm}^{-3}$. Since the different theoretical curves are similar, only one theoretical profile (Ref. 1) has been included here. The profiles have been normalized to have the same half-width and average peak height. The D-Ar⁺ points (open circles) near the peaks are practically indistinguishable from the H-H⁺ points; for the rest of the profile, they are very close to the H-Ar⁺ (broken) line, so that they have been omitted for clarity.

es, the density dependence becomes more like that predicted by the theories. The values extrapolated to $\mu = \infty$ approach quite closely the magnitude and density dependence of the theoretical values.

Figure 8 also contains all other experimental data on the H_β dip known to us. These values are indicated by circles around the appropriate symbol for μ (dots for $\mu = 0.5$, etc.); as a special case, the numerous data of Hey¹² are enclosed by a box. Our own data, from Ref. 7, are left uncircled. The results of Hey, which were measured for an effective μ of about 0.6, are somewhat lower than our and the other results, particularly at lower electron densities. A significant part of the discrepancy may be due to end-layer effects in Hey's shock tube. Indeed, this author derives a model for the helium end layer and concludes it is plausible that the total difference between his results and the Kepple-Griem calculated values could be due to such an effect. One should also note that the data points of Hey corresponding to $\mu \approx 1$ fall in among his points for $\mu \approx 0.5$. Thus, his results do not confirm our observation of the reduced-mass dependence of the H_β dip. These points aside, the agreement between different experimental values seems quite satisfactory.

V. H_γ

As with H_α and H_β , less structure is observed near the line center of H_γ than theoretically pre-

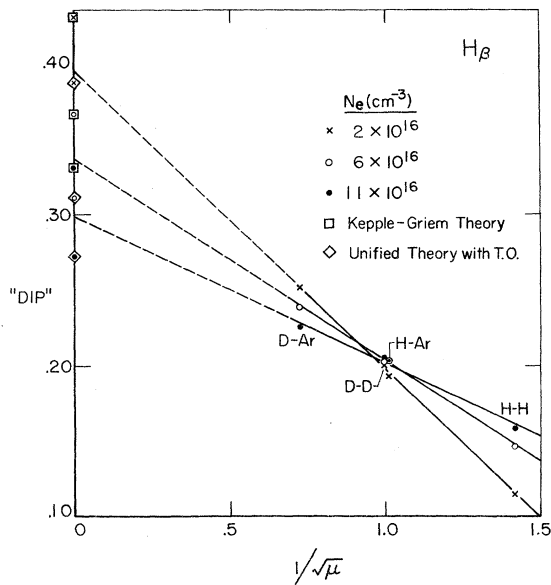


FIG. 7. "Dip" of H_β versus the inverse square root of the reduced mass at three different values of electron density. The extrapolation is made by assuming that the observed straight-line dependence continues to $\mu = \infty$.

dicted. The calculated profiles^{1,2} exhibit pronounced "shoulders" which stem from a depression in the profile that is deepest at about $\frac{3}{4}$ of peak intensity. The underlying physical cause is the absence of strong Stark components at this part of the profile. However, as can be seen in Fig. 9, the experimental profile measured in pure hydrogen ($\mu = 0.5$) exhibits practically no shoulders. The experimental profile with the largest reduced mass ($\mu = 2$), D-Ne, shows distinct structure near the $\frac{3}{4}$ -width, though still much less than the theoretical profile.

The experimental procedure was essentially the same as for H_β . The pure-hydrogen and -deuterium profiles were measured side-on utilizing the Abel inversion. The H-Ne⁺ and D-Ne⁺ profiles (Argon could not be used because of line interference in the H_γ region) were measured end-on using small ($\approx 4\%$) admixtures of hydrogen or deuterium to neon. Pure-neon gas was kept in the electrode regions, and the electron density was measured from the half-width of H_γ . The optical depth was determined by comparing the measured absolute

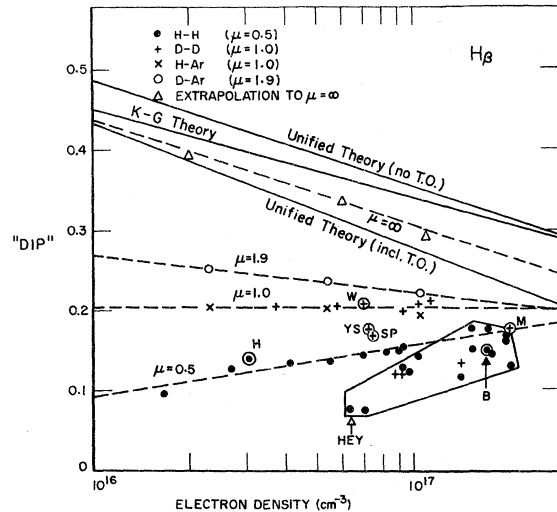


FIG. 8. Dip of H_β versus electron density for four different values of the reduced mass, including values extrapolated to $\mu = \infty$. The experimental data points are primarily from our previous paper (Ref. 7) (all points for $\mu = 0.5, 1,$ and 1.9 not enclosed by a circle or box). In addition, results are included from measurements by Hill *et al.*, Ref. 5 (marked H); Hey, Ref. 12 (data inside box); Behringer, Ref. 13 (B); Morris and Krey, Ref. 14 (M); Shumaker and Popenoe, Ref. 15 (SP); Yokley and Shumaker, Ref. 16 (YS); and Wende, Ref. 17 (W). Also included are values for the dip calculated by Vidal, Cooper, and Smith, Ref. 1 (unified theory, no time ordering); Roszman, Ref. 10 (unified theory, time ordering included); and Kepple and Griem, Ref. 2 (KG theory). Temperatures for our data and for the theoretical curves range from 10 000 K at $N_e = 10^{16}$ to 13 000 K at $N_e = 10^{17}$.

intensity at the line peak with that calculated for a blackbody at that wavelength and at the arc temperature. Numerical values for τ were found to be 0.02 or less, so that no corrections were necessary. Other critical experimental factors were checked with techniques like those discussed for H_α . However, for the H_γ studies these factors are not nearly as important as for H_α since no area normalization is involved and the width ratio is only weakly dependent on electron density.

To put the results observable in Fig. 9 on a more quantitative basis, the ratio of $\frac{3}{4}$ - to $\frac{1}{2}$ -width was measured over a range of electron densities. The results are plotted in Fig. 10 for the three experimentally obtainable reduced masses. The theoretical ratios (no time-ordering calculations are available for this line) are also included for comparison: a pronounced "depression" around the $\frac{3}{4}$ -width results in the theoretical ratios being much smaller.

We have taken from Fig. 10 the data at $N_e \approx 4 \times 10^{16} \text{ cm}^{-3}$, where they are most plentiful, and have plotted the $\frac{3}{4}$ - to $\frac{1}{2}$ -width ratio versus $1/\sqrt{\mu}$ in Fig. 11 in a manner analogous to the H_β case (Fig. 7). The data do not fall on a straight line, so that there is no satisfactory means available for extrapolating them to $\mu = \infty$. The curve appears to flatten out at larger $1/\sqrt{\mu}$, which could be due effectively to a saturation which occurs at small reduced masses. In other words, for $\mu \lesssim 1$ the depression is already smeared out, and any further smearing will have little effect on the structure. Still, the general trends apparent in Figs. 10 and 11 seem to warrant the conclusion that the observed reduced-mass effect can account for a significant part of the dis-

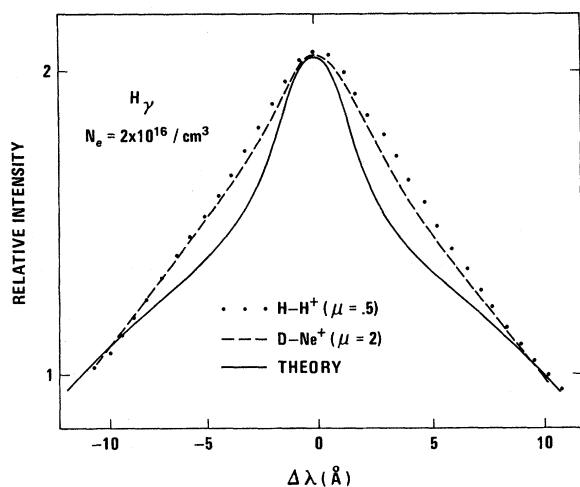


FIG. 9. Central part of the H_γ profile at two different values of the reduced mass. As with H_β , only one theoretical profile (Ref. 1) is included (the other one is very similar), and all profiles have been normalized to match at the peak and half-width.

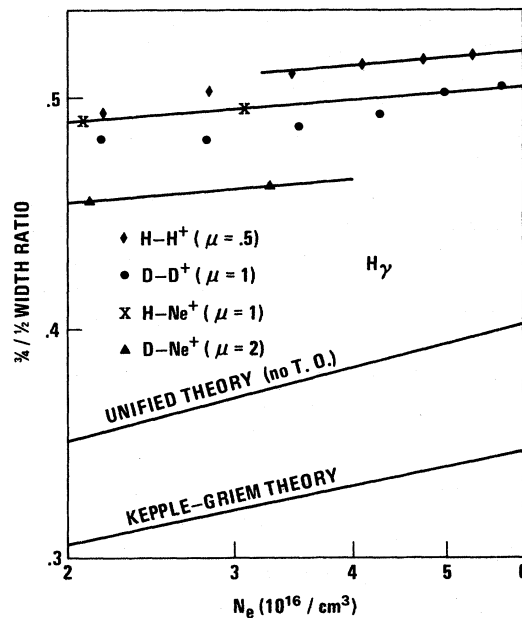


FIG. 10. Electron density dependence of the H_γ , $\frac{3}{4}$ - to $\frac{1}{2}$ -width ratio. The calculated values of Vidal, Cooper, and Smith (Ref. 1) (unified theory, no time ordering) and Kepple and Griem (Ref. 2) are included. Profiles including time ordering are not available for H_γ .

crepancy between theory and experiment at the H_γ shoulder.

VI. H_δ

As for H_β , there is no unshifted central Stark component in the case of H_δ . The theory² therefore

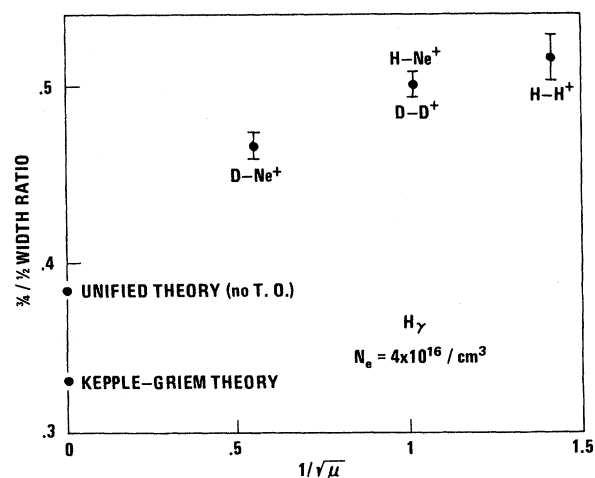


FIG. 11. Reduced-mass dependence of the H_γ , $\frac{3}{4}$ - to $\frac{1}{2}$ -width ratio at $N_e \approx 4 \times 10^{16} \text{ cm}^{-3}$. The calculated values of Vidal, Cooper, and Smith (Ref. 1) (unified theory, no time ordering) and Kepple and Griem (Ref. 2) are included.

predicts a small dip in the line center, similar to the one for H_β but less pronounced. The only experiment where this dip has been observed is the one of Hill, Gerardo, and Kepple.⁵ In another arc experiment⁴ and the present one, no dip has been found.

For three different reduced masses, profiles of H_δ have been measured. In pure hydrogen the measurements have been done side-on. For the mixtures H-Ar⁺ and D-Ar⁺, end-on measurements were made with a relatively high admixture of about 10% (by volume) of H₂ or D₂ to argon in order to obtain sufficient signal; thus for our plasma conditions, the relative concentration of hydrogen (or deuterium) ions was estimated to be about 30%. This gives rise to an "effective" reduced mass (μ_{eff}) of 0.85 and 1.7 for the H-Ar and D-Ar mixtures, respectively. (μ_{eff} is simply a weighted average, e.g., for the H-Ar mixture with the above hydrogen ion concentration, $\mu_{\text{eff}} = 0.3\mu_{\text{H-H}^+} + 0.7\mu_{\text{H-Ar}^+}$.) Figure 12 shows a comparison of the experimental line profiles with the theoretical profile obtained from the Kepple-Griem tables (no corresponding VCS profile is available). In the pure-hydrogen case the line has a clear maximum which flattens out and broadens with increasing μ . However, no distinct dip can be seen. A slight asymmetry favoring the blue side of the line center, analogous to the asymmetry in the H_β peaks, is observed for all experimental profiles.

The profiles of Fig. 12 are all area normalized at the same electron density. However, the uncertainty in the profile normalizations is quite large in this case, due primarily to the substantial continuum and H_ϵ contributions which had to be subtracted out. (The much smaller H_γ contribution was not considered.) Also, the electron density for the profile measured in pure hydrogen could be as much as 10% different from that measured for the H- (or D-) Ar mixtures since different diagnostic techniques were applied. As a result, no reliable comparison of the relative peak heights of half-widths could be made between the pure-hydrogen plasma and the two mixtures. On the other hand, the decrease in peak intensity from the H-Ar⁺ to the D-Ar⁺ case is felt to be reliably established since the mixture diagnoses and profile corrections were performed in an analogous manner for these two cases.

VII. DISCUSSION

With respect to possible distorting factors on the Stark profiles, we have not yet considered the possibility of fluctuations in temperature and electron density in stabilized arcs. Such possible lack of temporal homogeneity has been proposed by

Griem¹⁸ as a conceivable reason for the discrepancies near the line centers. To date, no direct observation with sufficient space and time resolution could be made which can confirm or disprove the existence of such "microinstabilities." However, there is considerable evidence to suggest that any microinstabilities which may be present in the arc source are not significantly responsible for the observed discrepancies with the theoretical profiles. Three such indications, all pertaining to the H_β measurements, are as follows:

(i). The H_β dip (for a given T , N_e , and μ) was observed to be independent of the physical properties of the plasma. For example, the H_β dip measured in a 96%-Ar-4%-H arc was essentially the same as that measured in a pure-deuterium arc. These two plasmas correspond to the same reduced mass ($\mu = 1$), but differ greatly in their electrical and thermal conductivity, in electric field strength, and in radial temperature and density gradients. Presumably, the development of any microinstability would be influenced by these physical properties.

(ii). The H_β dips measured in different plasma sources, including those with no applied electric fields, generally differ from one another much less than they differ from theoretical values. This is apparent in Fig. 8.

(iii). A relatively sensitive "homogeneity monitor" is provided by the ratio of the H_β peak-separation to its half-width. This value is computed to be 0.35 and 0.37, respectively, by the Vidal-Cooper-Smith¹ and the Kepple-Griem² theories and is practically independent of electron density. For $N_e \geq 10^{16}$ cm⁻³, our measurements yielded

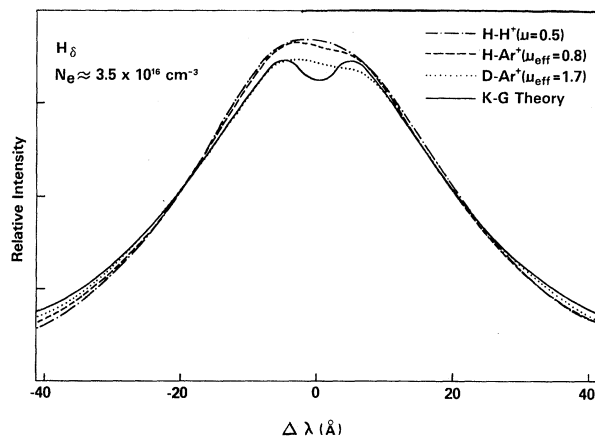


FIG. 12. Theoretical and experimental H_δ profiles for $N_e \approx 3.5 \times 10^{16}$ cm⁻³ and $T \approx 11000$ K. All profiles are area normalized. The H-Ar⁺ and D-Ar⁺ mixtures were both diagnosed and the profile corrections carried out in an analogous manner.

0.36, i.e., practically the same ratio, with the notable exception that the ratio was substantially reduced in cases where the plasma was not homogeneous. For example, this was observed whenever hydrogen or deuterium was permitted to enter the (cooler) electrode regions in end-on observations or when the arc channel was purposely made too wide, so that the arc was not sufficiently well stabilized. In that case kinks or bows occurred in the column.¹⁹ One would expect that any micro-instability which significantly affected the core of the profile would likewise cause a reduction in the above ratio from the theoretical value.

It should be added here that *both* end-on and side-on measurements were made of the dip in H_β . The end-on and side-on results agreed to within the experimental uncertainty of about 5% (of the dip).

Of course, none of the above indications can conclusively eliminate the possibility that the main reason for the discrepancy near the line center between experiment and theory is due to some problem with the experiments, but this should be related to the atom-ion reduced mass.

As of this writing, no theory exists which explains the reduced-mass dependences we have observed. Several different approximate theoretical treatments of H_β predict small or negligible ion dynamic effects. These include the recent work by Griem,²⁰ Hey,¹² Lee,²¹ and Capes, Stamm, and Voslamber.²² (A recent calculation by Cooper, Smith, and Vidal²³ has not been included in this list because their validity criteria are violated for $N_e > 10^{15}$ cm⁻³.) Each of these calculations utilizes various different approximations, such as a restriction to binary collisions or a finite series expansion of exponentials involving the time. It is at present an open question whether a more rigorous calculation will predict a more significant ion dynamic effect.

VIII. CONCLUSIONS

Variations in the central parts of the first four Balmer lines have been observed which depend in a systematic manner on the reduced mass of the radiating atom and perturbing ion.

The relative minimum or dip of H_β at a fixed electron density (and, approximately, fixed temperature) appears to scale linearly with $1/\sqrt{\mu}$, where μ is the atom-radiator-ion-perturber re-

duced mass. Both the magnitude of the relative minimum of H_β and the slope of its density dependence approach the values predicted by the current theories as μ is increased. Values extrapolated to infinite reduced mass approach the theoretical values quite closely.

For H_α , the half-width as well as the normalized peak height are also observed to depend on the reduced mass at constant N_e and T . This dependence increases slightly at lower electron densities. If a $1/\sqrt{\mu}$ dependence is assumed, the half-width values extrapolated to $\mu = \infty$ are in close agreement with recent "unified-theory" calculations that include time ordering.

In the case of H_γ , the absence of pronounced shoulders near the line core appears to be due, at least in part, to the dependence on finite reduced mass.

For H_δ , a plateau at the line center is observed to broaden with reduced mass. However, the distinct central minimum predicted by theory is not observed.

The physical reason for the observed reduced-mass dependence has not yet been established. In fact, recent theoretical treatments of ion dynamics predict very small or negligible effects. It is therefore of interest to perform further studies on the Balmer lines. It would be especially interesting to check whether the observed effects scale as the relative radiator-perturber velocities, as suggested by the approximate $1/\sqrt{\mu}$ dependence. In this case one would really expect a $(T/\mu)^{1/2}$ dependence, which we could not check since we worked with all plasmas in the same very narrow temperature range. A measurement of the temperature dependence at constant N_e and μ would thus be very desirable in this regard. Attempts by us in this direction have not been successful as yet because we have been unable to obtain sufficient temperature variation with the arc source.

ACKNOWLEDGMENTS

We wish to thank A. Smith for his assistance with the data reduction and Dr. L. Roszman for providing us with the results of his calculations prior to publication. We also appreciate the assistance of D. Paquette with the electronics. One of us (V.H.) would like to thank the Deutsche Forschungsgemeinschaft for the support during his stay at the National Bureau of Standards.

*Permanent address: Institut für Experimentalphysik, Universität Kiel, Kiel, Germany.

¹C. R. Vidal, J. Cooper, and E. W. Smith, *Astrophys. J. Suppl.* **25**, 37 (1973).

²P. Kepple and H. R. Griem, *Phys. Rev.* **173**, 317 (1968); numerical profiles appear in: H. R. Griem, *Spectral Line Broadening by Plasmas* (Academic, New York, 1974).

- ³D. Voslamber, Z. Naturforsch. A 24, 1458 (1969).
- ⁴W. L. Wiese, D. E. Kelleher, and D. R. Paquette, Phys. Rev. A 6, 1132 (1972).
- ⁵R. A. Hill, J. B. Gerardo, and P. C. Kepple, Phys. Rev. A 3, 855 (1971).
- ⁶D. D. Burgess, J. Phys. B 3, L70 (1970); J. W. Dufty, Phys. Rev. A 2, 534 (1970).
- ⁷D. E. Kelleher and W. L. Wiese, Phys. Rev. Lett. 31, 1431 (1973).
- ⁸H. Ehrich and H. J. Kusch, Z. Naturforsch. A 28, 1794 (1973).
- ⁹D. Voslamber, Abstract: G8, Program and Abstracts for the Second International Conference on Spectral Lines, University of Oregon, 1974 (unpublished).
- ¹⁰L. J. Roszman, Phys. Rev. Lett. 34, 785 (1975).
- ¹¹M. C. Lortet and E. Roueff, Astron. Astrophys. 3, 462 (1969).
- ¹²J. D. Hey, University of Maryland Report No. 74-089 (unpublished).
- ¹³K. Behringer, Z. Phys. 246, 333 (1971).
- ¹⁴J. C. Morris and R. U. Krey, Phys. Rev. Lett. 21, 1043 (1968).
- ¹⁵J. B. Shumaker, Jr. and C. H. Popenoe, Phys. Rev. Lett. 21, 1046 (1968).
- ¹⁶C. R. Yokley and J. B. Shumaker, Rev. Sci. Instrum. 34, 551 (1963).
- ¹⁷B. Wende, Z. Naturforsch. A 22, 181 (1967).
- ¹⁸H. R. Griem, Comments At. Mol. Phys. 3, 181 (1972).
- ¹⁹W. L. Wiese, Proceedings of the VII Yugoslav Symposium on Physics of Ionic Gases, 1974 (unpublished).
- ²⁰H. R. Griem, Comments At. Mol. Phys. 2, 19 (1970).
- ²¹R. J. Lee, J. Phys. B 6, 1060 (1973).
- ²²H. Capes, R. Stamm, and D. Voslamber, in Ref. 9, Abstract: G6.
- ²³J. Cooper, E. W. Smith, and C. R. Vidal, J. Phys. B 7, L101 (1974).